

## PREPARATION OF CORE FOAMED Al PANELS

Varužan Kevorkijan<sup>1\*</sup>, Uroš Kovačec<sup>2</sup>, Irena Paulin<sup>3</sup>, Srečo Davor Škapin<sup>4</sup>,  
Monika Jenko<sup>3</sup>

<sup>1</sup>*Independent Researcher, Betnavska cesta 6, 200 Maribor, Slovenia*

<sup>2</sup>*Impol Aluminium Industry, Partizanska 38, 2310 Slovenska Bistrica, Slovenia*

<sup>3</sup>*Institute of Metals and Technology, Lepi pot 11, 1000 Ljubljana, Slovenia*

<sup>4</sup>*Institut "Jožef Stefan", Jamova 39, 1000 Ljubljana, Slovenia*

*Received 20.08.2011*

*Accepted 27.09.2011*

### Abstract

In this paper, laboratory and semi-industrial processes for the preparation of aluminium foam samples and core-foamed panels with closed porosity were investigated. The samples were prepared starting from the accumulative hot-roll bonded precursors, with titanium hydride (TiH<sub>2</sub>) or dolomite (Ca<sub>0.5</sub>Mg<sub>0.5</sub>CO<sub>3</sub>) powder added as the foaming agent. The formation of the precursors was performed in three steps. In the initial stage, titanium dihydride or dolomite particles were deposited on a single side of a selected number of aluminium strip samples made from the alloy AA 1050. In the second step, by putting together in pairs, single-sided coated strips, precursors with a two-layered structure were prepared. The samples were hot-rolled to a final thickness of 1.9-3.8 mm, introducing a total deformation of about 45-49% by a process well-known as accumulative hot-roll bonding. In the third stage of the precursor's formation, the desired multilayered precursor's structure was achieved by hot-roll multi-passing, i.e., by repeating (with 2-16 passes) the accumulative hot-roll bonding procedure. The obtained precursors were foamed in an electrical furnace, under different foaming conditions, based on the initial temperature of the thermal decomposition of the foaming agent. The microstructure of the obtained foam samples was investigated with optical and scanning electron microscopy. According to the accumulated experimental results, one can conclude that the usage of dolomite powder as a foaming agent with a higher temperature of thermal decomposition (>750 °C) compared to TiH<sub>2</sub>, which thermally decomposed even at the temperature of hot-rolling (>350 °C), enabling the formation of multilayered precursors at higher temperatures of hot-rolling without any intermediate annealing. This consequently increases the productivity of the foamed core panel production without influencing their final quality.

---

\* Corresponding author: Varužan Kevorkijan, [varuzan.kevorkijan@impol.si](mailto:varuzan.kevorkijan@impol.si)

*Key words: Al foams, core foamed Al panels, precursors preparation, accumulative hot-roll bonding, comparison of different foaming agents, characterisation*

### Introduction

Accumulative Roll Bonding (ARB) is a new and promising manufacturing process for closed-cell aluminium foams and core-foamed panels [1-3]. The ARB process, as one of the severe plastic deformation processes, has been applied to many metals and alloys to produce an ultra-fine crystal grain structure. The processing procedure is presented in Fig.1.

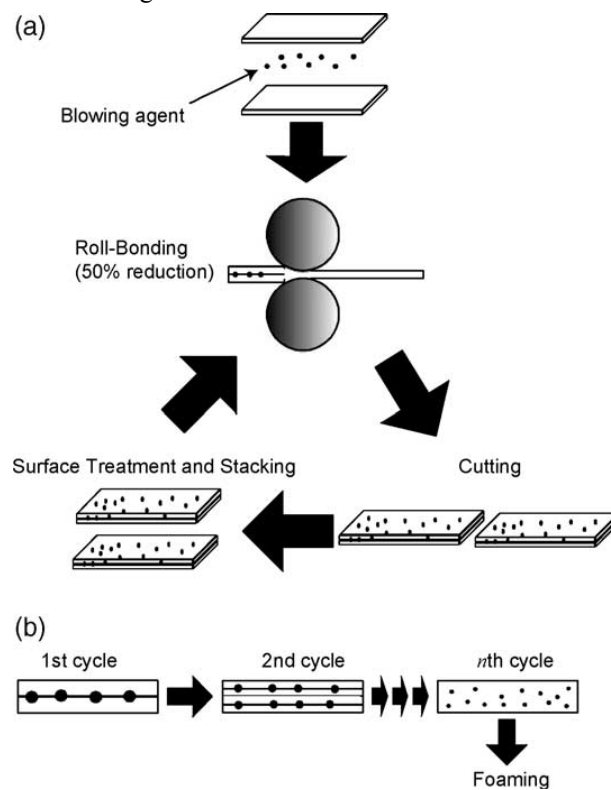


*Fig.1. (a) Schematic illustration of the manufacturing process of a precursor sheet using the ARB process. (b) Prediction of gradual distribution of added foaming-agent particles [3].*

Instead of aluminium powder, aluminium sheet is applied as a starting material, making this processing route cost-effective and promising for further industrialization. During the first stage, two aluminium strips are stacked with the appropriate amount of selected blowing-agent powder of the proper morphology. Second, the strip is roll-bonded by a 50% reduction and cut into two. After repeatedly covering the surface with blowing agent, the two strips are stacked to be the initial dimension, and then roll-bonded again. Since these procedures can be repeated indefinitely, the desired

multilayered precursor's structure could be achieved. By multiplying the foaming-agent layers, its uniform distribution across the entire cross-section of the prepared precursor can be achieved. Finally, the obtained precursors are foamed to the end products: foamed aluminium sheet or core-foamed panels.

Investigations performed in the past few years have confirmed the great potential of the ARB processing route in the cost-effective and highly productive fabrication of foamed aluminium sheets and various core-foamed panels by titanium hydride ( $\text{TiH}_2$ ) as a foaming agent [3, 4]. An additional reduction in cost can be achieved by replacing the expensive  $\text{TiH}_2$  with alternative, inexpensive foaming agents, particularly carbonates, among which natural carbonates such as  $\text{CaCO}_3$  marble powder or  $\text{CaMg}(\text{CO}_3)_2$  dolomite powder are particularly attractive.

Successfully replacing the  $\text{TiH}_2$  with carbonates in the foaming precursor fabricated by the powder metallurgical or stir-casting route has been reported by several authors [5-9]. However, similar investigations of replacing the  $\text{TiH}_2$  foaming agent with dolomite particles in accumulative hot-roll bonded precursors are still not completed. Therefore, the purpose of this work was to investigate the possible benefits of replacing  $\text{TiH}_2$  with dolomite particles in multilayered precursors made by ARB.

### Experimental procedure

The samples were prepared by starting from the accumulative hot-roll bonded precursors, with  $\text{TiH}_2$  or dolomite ( $\text{Ca}_{0.5}\text{Mg}_{0.5}\text{CO}_3$ ) powder added as the foaming agent.

The formation of the precursors was performed in three steps. In the initial stage  $\text{TiH}_2$ , or dolomite particles were deposited on a single side of a selected number of aluminium strip samples (100mm in width, 200 mm in height and with a thickness approximately 2-4 mm) made from AA 1050 alloy. The suspension of the powdered foaming agent ( $\text{TiH}_2$  or  $\text{CaMg}(\text{CO}_3)_2$ ) in acetone was spread out on the strip with a painter's roll.  $\text{TiH}_2$  (supplier: AG Materials Inc.) and  $\text{Ca}_{0.5}\text{Mg}_{0.5}\text{CO}_3$  (supplier: Granit d.o.o., Slovenska Bistrica, Slovenia) were applied as foaming agents. The average particle size of the powders used in the experiments is listed in Table 1. The particle size distribution of the powdered foaming agents was measured using laser particle analyzer (Malvern Mastersizer 2000). The relative error of the measurement was within  $\pm 1\%$ .

The surface concentration of the foaming agent achieved after evaporation the acetone was between approximately  $2.5 \times 10^{-3}$  and  $3.5 \times 10^{-3}$   $\text{mg}/\text{mm}^2$ . In the second step, by putting together in pairs single-sided coated strips, precursors with a two-layered structure were prepared. The samples were hot-rolled to a final thickness of 1.9-3.8 mm, introducing a total deformation of about 45-49% by a process that is well known as accumulative hot-roll bonding. It was found that the consistency of the obtained precursors (the adhesion between two layers) was strongly affected by the parameters of the hot-rolling (the strip deformation and the temperature of the hot-rolling). These were significantly limited by the technical possibilities of the existing mini hot-rolling mill. The diameter of the working rolls was only 200-450 mm. However, by carefully selecting the optimal power of the hot-rolling mill unit (about 18-50 kW) for the proper deformation of the strip and the temperature of the hot-rolling (between 300-350°C), the complete recrystallization of the strip was achieved, avoiding in that way any possible hardening of the wrought aluminium. In the third stage of the precursor formation, the

desired multilayered precursor structure was achieved by hot-roll multi-passing, i.e., by repeating (with 2-16 passes) the accumulative hot-roll bonding procedure. By the multiple accumulative hot-roll bonding and by doubling the layers of the foaming agent, its uniform distribution was achieved across the entire cross-section of the prepared precursors.

Table 1. The average particle size and the cumulative particle size distribution of the  $TiH_2$  and dolomite powder applied as foaming agents.

TiH <sub>2</sub> powder	TIH-0420
Average particle size (μm)	20.4
Cumulative particle size distribution (μm)	
D <sub>10</sub>	13.1
D <sub>25</sub>	17.4
D <sub>50</sub>	20.4
D <sub>75</sub>	23.7
D <sub>90</sub>	41.4
Uniformity of particle size distribution (μm)	
D <sub>90</sub> -D <sub>10</sub>	28.3
Dolomite powder	D-4
Average particle size (μm)	20.8
Particle size distribution	
D <sub>10</sub>	11.2
D <sub>25</sub>	15.9
D <sub>50</sub>	20.8
D <sub>75</sub>	23.1
D <sub>90</sub>	27.2
Uniformity of particle size distribution (μm)	
D <sub>90</sub> -D <sub>10</sub>	16.0

The precursors were foamed in a conventional batch electrical furnace with air-atmosphere circulation under various experimental conditions (time, temperature) and by applying the same cooling method. Before foaming, the individual precursors were placed on a ceramic plate covered by a boron nitride layer. The plate dimensions and the precursor size (100 x 100 mm) were selected to allow the complete expansion of the precursor to foam. The arrangement was placed inside a pre-heated batch furnace at a selected temperature and held for the selected holding time. In samples with  $TiH_2$ , thermal decomposition was observed, starting from approximately 350 °C. These samples were foamed at 700-750 °C, for 3-18s. Samples with the dolomite foaming agent, for which the thermal decomposition is initiated above 750 °C, were foamed at 780 °C for 2-5 min. After that, the sample was removed from the furnace and the foaming process was stopped by rapid cooling with pressurised air to room temperature. The thermal history of the foam sample was recorded, using a thermocouple located

directly in the precursor material. The density of the foam was calculated using Archimedes method. The porosity of the manufactured foam was calculated by formula:  $1 - (\text{foam density} / \text{aluminium density})$ . Macro and microstructural examinations were performed on sections obtained by wire precision cutting across the samples and on samples mounted in epoxy resin, using optical and scanning electron microscopy (SEM/EDS). The average pore size of the pores in the foams was estimated by analysing optical and scanning electron micrographs of the as-polished foam bars using the point-counting method and image analysis and processing software.

### Modelling of the surface concentration and morphology of the foaming agent in ARB precursors

In precursors fabricated by the ARB processing route, the proper surface concentration and morphology of the foaming agent are crucial for the development of high-quality foams with closed cells and a uniform microstructure. Because of that, it is very important to correlate the surface concentration and morphology of the foaming agent with an average cell size and microstructure of the foam.

The particles of foaming agent are, as much as possible, homogeneously dispersed on the surface of the aluminium sheet, as is evident in Fig. 2.

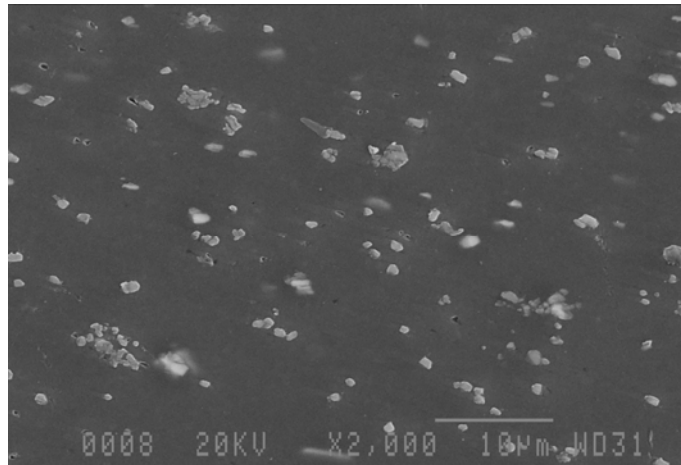


Fig.2. SEM micrograph of the surface of an aluminium sheet after the first cycle of ARB, with homogeneously distributed dolomite particles.

The neighbouring particles of foaming agent are mutually apart for an average minimum distance,  $X_{\min}$ . As will be demonstrated in the model, this distance is determined by the surface concentration of the foaming agent,  $C$ , and its average particle size,  $d_{50}$ .

The surface concentration of the foaming agent is defined as follows:

$$C = m/S \quad (1)$$

Here,  $m$  is the total mass of the foaming agent and  $S$  is the surface of the aluminium sheet. The molar surface concentration,  $C'$ , is defined as:

$$C' = m/(MS) \quad (2)$$

where M represents the molar mass of the selected foaming agent. Finally, the particle surface concentration,  $C''$ , is introduced as:

$$C'' = N/S = 1/X_{min}^2 \quad (3)$$

N is the total number of particles of foaming agent:

$$N = m_p/M = d_{50}^3 \pi \rho / 6M \quad (4)$$

In Eq. 4,  $m_p$  represents the mass of an average particle of foaming agent,  $d_{50}$  is the average particle size and  $\rho$  is the theoretical density of the foaming agent.

Therefore, by combing Eqs.1-4 we can derive, for the particle surface concentration, the following expression:

$$C'' = 6C/(d_{50}^3 \pi \rho) \quad (5)$$

and, consequently, for  $X_{min}$ :

$$X_{min} = [(d_{50}^3 \pi \rho) / 6C]^{1/2} \quad (6)$$

Applying, for the bubbles growth, a simple, stoichiometric model, in which the complete thermal decomposition of an individual foaming agent particle provides a gas phase for the bubble nucleation and growth, the maximum bubble diameter,  $D_{max}$ , can be determined with the ideal gas equation:

$$p_{max}V = nRT \quad (7)$$

where n corresponds to the number of moles of gas phase inside the bubble, V is the bubble volume and T is the temperature.

$p_{max}$  can be calculated by applying Laplace's equation:

$$p_{max} = (2\sigma_{lg}/r) + \rho gh + p_0 \quad (8)$$

The maximum bubble pressure,  $p_{max}$ , is the sum of the capillary ( $2\sigma_{lg}/r$ ), hydrostatic ( $\rho gh$ ) and atmospheric ( $p_0$ ) pressures. The capillary pressure depends on the surface tension,  $\sigma_{lg}$ , at the gas-liquid interface and the bubble radius (r); the hydrostatic pressure is determined by the immersion depth (h) and the density of the molten aluminium alloy ( $\rho$ ).

By considering a spherical bubble and combining Eqs. (7) and (8), we can calculate:

$$[(2\sigma_{lg}/r) + \rho gh + p_0] (4/3)r_{max}^3 \pi = nRT \quad (9)$$

During an early stage of the bubble growth, only the capillary pressure ( $2\sigma_{lg}/r$ ) should be considered, while in the final stage of the bubble's growth the only important pressure is the atmospheric ( $p_0$ ). Note that for laboratory conditions, the hydrostatic pressure ( $\rho gh$ ) is always negligible.

Based on this, in the case considered by the model:

$$p_{max} = p_0 \quad (10)$$

Therefore, the maximum bubble diameter,  $D_{max}$ , is finally determined by the formula:

$$D_{max} = d_{50}[(kRT\rho)/p_0M]^{1/3} \quad (11)$$

Here, k represents the stoichiometric constant (k = 1 for TiH<sub>2</sub> and k=2 for dolomite). In Tables 2 and 3, the calculated values for the maximum bubble radius for cells grown from the TiH<sub>2</sub> and dolomite particles of different initial particle size are listed.

Table 2. Maximum bubble radius for a cell grown from TiH<sub>2</sub> particles with different initial particle sizes ( $d_{50}$ ).

The average particle size of TiH <sub>2</sub> ( $\mu\text{m}$ )	3	20	40	75	140
Maximum bubble diameter, $D_{max}$ ( $\mu\text{m}$ )	54	360	808	1.352	2.526

Table 3. Maximum bubble radius for bubbles created by dolomite particles of different initial particle sizes ( $d_{50}$ ).

The average particle size of dolomite ( $\mu\text{m}$ )	3	5	10	20	35
Maximum bubble diameter, $D_{max}$ ( $\mu\text{m}$ )	40	68	132	268	468

According to the theoretical prediction based on Eq. 11, at the same initial particle size of the applied foaming agent and the same foaming conditions, the bubbles created by TiH<sub>2</sub> should be coarser.

In order to obtain a stable foam microstructure, with isolated closed cells, it is necessary that:

$$X_{min} > D_{50} \quad (12)$$

By combining Eqs.6, 11 and 12, the condition (12) leads to the required correlation between the surface concentration and the foaming-agent morphology:

$$C < const. (d_{50}/T)^{2/3} \quad (13)$$

Based on the model, it is evident that for the selected morphology of the foaming agent,  $d_{50}$ , and foaming temperature, T, the surface concentration of the foaming agent, C, cannot be selected arbitrarily, but, in order to achieve a foam microstructure with stable individual closed cells, it should fulfil the condition expressed by Eq.13.

## Results and discussion

### *Foam properties as a function of the composition of accumulative roll-bonded precursors*

The results of the investigation of the foam properties (density and cell size distribution) achieved by applying various types (TiH<sub>2</sub> or dolomite) and surface concentrations of foaming agents are reported in Tables 4 and 5.

Table 4. The experimentally measured density and cell-size distribution of the aluminium foam samples at various concentrations of  $TiH_2$  foaming agent. The foaming conditions: 700 °C, 120s.

Surface concentrations of $TiH_2$ (mg/mm <sup>2</sup> )	$2.5 \times 10^{-3}$	$3.0 \times 10^{-3}$	$3.5 \times 10^{-3}$
Density of Al foam (% T.D.)	25.9±1.3	23.8±1.2	21.2±1.1
Cell size distribution (mm)			
D <sub>10</sub>	2.6±0.3	3.2±0.3	3.3±0.3
D <sub>25</sub>	2.7±0.3	3.5±0.3	3.8±0.3
D <sub>50</sub>	2.8±0.3	3.7±0.4	5.1±0.5
D <sub>75</sub>	3.0±0.3	4.2±0.3	5.5±0.6
D <sub>90</sub>	4.6±0.5	8.4±0.3	10.4±1.0
Uniformity of cell size distribution (µm)			
D <sub>90</sub> -D <sub>10</sub>	2.0±0.2	5.2±0.6	7.1±0.7

Table 5. The experimentally measured density and cell-size distribution of aluminium foam samples at various concentrations of dolomite foaming agent. The foaming conditions: 700 °C, 120s.

Surface concentrations of dolomite (wt. %)	$2.5 \times 10^{-3}$	$3.0 \times 10^{-3}$	$3.5 \times 10^{-3}$
Density of Al foam (% T.D.)	15.4±0.8	12.8±0.6	11.1±0.6
Cell size distribution (mm)			
D <sub>10</sub>	2.0±0.2	2.4±0.2	2.9±0.3
D <sub>25</sub>	2.3±0.2	2.9±0.3	3.3±0.3
D <sub>50</sub>	2.5±0.3	3.2±0.3	4.7±0.5
D <sub>75</sub>	2.7±0.3	4.8±0.6	5.1±0.5
D <sub>90</sub>	5.8±0.6	7.6±0.8	9.7±1.0
Uniformity of cell size distribution (µm)			
D <sub>90</sub> -D <sub>10</sub>	3.8±0.4	5.2±0.5	6.8±0.7

Generally, the panels foamed with the dolomite foaming agent were with a more uniform cell-size distribution and lower average bubble size. The most uniform cell-size distribution was achieved in foam samples foamed with the minimum surface concentration ( $2.5 \times 10^{-3}$  mg/mm<sup>2</sup>) of dolomite powder, Fig. 3.

The experimentally determined values of the average bubble radius in the foamed panels were at least for one order of magnitude higher than those predicted by the model. The reason for that difference is in effects limiting the stability of the individual bubbles, which are not considered by the model. These effects are as follows: bubble flow, drainage, rupture or coalescence and coarsening.

From the difference between the theoretically predicted and experimentally determined values of the bubble radius, it is possible to estimate the stability of the real foam systems considered in this work. The experimental findings clearly confirm that coarser bubbles are more stable than finer ones. In addition, it is also evident that the stability of the bubbles is much higher in foams created by dolomite particles than in the counterparts foamed by  $\text{TiH}_2$ . However, in both cases the average bubble sizes are proportional to the average initial size of the foaming particles – finer foaming particles lead to finer bubbles, while coarser ones lead to larger bubbles, as was predicted by the model.

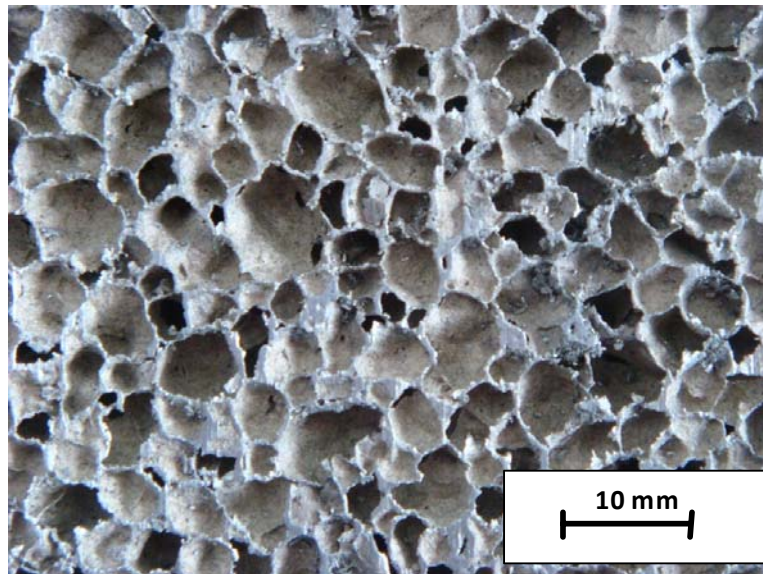


*Fig. 3. The homogeneous microstructure of the Al foam made from the ARB precursor with dolomite particles as the foaming agent. The ARB precursor was made by four roll-bonding cycles.*

On the other hand, the density of the aluminium foam samples was inversely proportional to the bubble radius: the foam samples with finer bubbles had the higher density and, in contrast, the foam samples with larger bubbles were densely lighter. At the same time and under the same foaming conditions (temperature, time), the foams made with the dolomite possessed a significantly lower density than the samples with similar cell size foamed by the  $\text{TiH}_2$ .

As is evident from the cell-size distribution data listed in Tables 4 and 5, an increase of the foaming-agent surface concentration (either  $\text{TiH}_2$  or dolomite) leads to the formation of foams with larger bubbles and a lower density. However, also in that case, the samples foamed with dolomite were with smaller bubbles and lower densities.

The experimentally developed foam microstructures were mostly influenced by the degree of foam movement slowing down (i.e., the foam stability) attained in particular trials. In addition, the microstructure of foams was also influenced in some cases by the layered structure of the ARB precursors.

The slowing down of the movement of the foam includes the prevention of flow (the movement of bubbles with respect to each other caused either by external forces or changes in the internal gas pressure during foaming), drainage (flow of liquid metal through the foam), coalescence (sudden instability in a bubble wall leading to its disappearance) and coarsening (slow diffusion of gas from smaller bubbles to bigger ones).

The layered structure of the ARB precursors caused, in some samples, the appearance of so-called “line segregation”, i.e., the flow of liquid metal across the line, Fig.4. Such segregation is most probably involved in the non-sufficient and/or different plastic deformation of individual layers during various roll-bonding cycles.

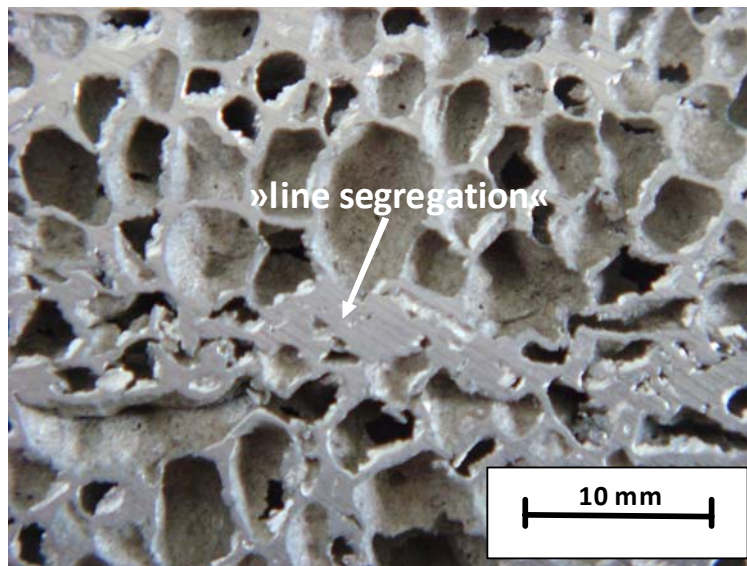


Fig. 4. The characteristic “line segregation” in the samples of aluminium foams made from ARB precursors using dolomite as a foaming agent.

Generally, the foam stability in the liquid and semi-solid state of an aluminium alloy is improved by increasing the thickness of the bubble wall, decreasing the surface tension of the molten metal and increasing its viscosity. Simultaneously decreasing the surface tension and increasing the viscosity of molten aluminium can be achieved by introducing to the molten metal some amount of ceramic particles, e.g. formed in situ, by the thermal decomposition of the foaming agent at the interface between molten aluminium and the gas phase.

Quantitatively, the foam stability in the liquid and semi-solid state might be expressed by a dimensionless foam-stability factor (FSF), which we defined as:

$$FSF = X_0 \eta / (\sigma t) \quad (14)$$

where  $X_0$  is the average distance between neighbouring bubbles (which is proportional to the wall thickness),  $\eta$  is the dynamic viscosity of the slurry,  $\sigma$  is the surface tension at the interface molten or semi-solid aluminium-gas and  $t$  is the foaming time.

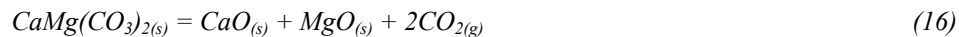
Evidently, a higher FSF means better foam stability. Unfortunately, in practice, it is not easy to determine the viscosity and the surface tension of the slurry of the molten aluminium alloy and the foaming agent particulates as well as the wall thickness of bubbles during their growth. Because of that, the usage of FSF is mostly limited to theoretical and, to some level, qualitative considerations.

The main difference between the  $TiH_2$  and the dolomite foaming agent, which influences the foam microstructure development, is the following: (i) in the nature and reactivity of products of its thermal decomposition and (ii) the temperature interval of thermal decomposition.

In ARB precursors with  $TiH_2$ , the thermal decomposition of the foaming agent was observed starting from approximately 350 °C. The  $TiH_2$  decomposes to  $Ti_{(s)}$  and  $H_{2(g)}$ , Eq. 15, which do not tends to react with molten aluminium in the way of creating secondary ceramic phases making it possible to slow down the movement of the foam. Because of that, the internal surface of the bubble wall foamed by the  $TiH_2$  is clean (Fig. 5b).



In contrast to this, the thermal decomposition of the dolomite foaming agent, Eq. (16), proceeded above 700 °C, resulting in highly reactive products:  $MgO_{(s)}$ ,  $CaO_{(s)}$  and  $CO_{2(g)}$  [7].



$CaO$  and  $MgO$  are in the form of solid particulate aggregates, appearing at the molten metal- $CO_{2(g)}$  interface, while  $CO_{2(g)}$  reacts with the molten aluminium in a bubble covering bubble internal surface with a thin, mostly continuous, film of  $Al_2O_3$  (Fig. 5a). Therefore, all the products of the dolomite thermal decomposition ( $MgO$ ,  $CaO$  and  $Al_2O_3$ ) are very effective in slowing down the foam movement, decreasing the surface tension and increasing the local viscosity of the slurry. Due to the limited foam movement, bubbles in solidified samples remain significantly finer, resulting in foams with a higher density (a lower volume fraction of bubbles).

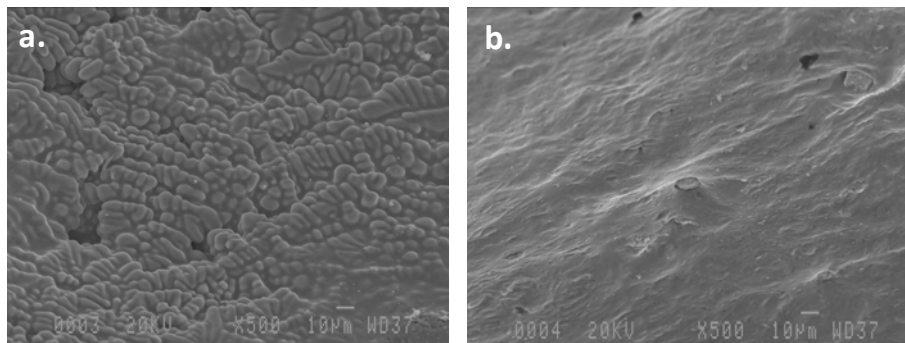


Fig. 5a, b. SEM micrograph of the internal surface of the bubble wall: (a) bubble wall fully covered by  $Al_2O_3$ ,  $CaO$  and  $MgO$  particles in bubbles foamed by dolomite and (b) clean internal surface in bubbles foamed by  $TiH_2$ .

*Fabrication of prototype core-foamed aluminium panels*

Accumulative hot-roll bonded precursors with dolomite particles as a foaming agent were successfully foamed to core-foamed panels with a wall thickness of about 2 mm and a thickness of the foamed core of about 10 mm. The flat panel samples (approx. 150 mm long and 80 mm wide) were routinely foamed from the ARB precursors using the existing laboratory capabilities, Fig. 6.



*Fig. 6. The cross-section of the prototype core-foamed panel made from ARB precursor with dolomite particles as the foaming agent.*

**Conclusion**

Our experimental findings confirmed that the ARB procedure is very promising (semi)-industrial route for the production of precursors for core-foamed aluminium panels. By combining a pair of AA 1050 aluminium alloy strips and various foaming

agents (TiH<sub>2</sub> or dolomite powders), several foaming precursors were prepared through two to four cycles of ARB and successfully foamed into core-foamed aluminium panels.

The use of dolomite powder as a foaming agent with a higher temperature of thermal decomposition (>700 °C) compared to TiH<sub>2</sub>, which thermally decomposed even at the temperature of hot-rolling (>350 °C), enabled the formation of multilayered precursors at higher temperatures of the hot-rolling without any intermediate annealing. This significantly improved the productivity of the production of core-foamed aluminium panels without influencing their final quality.

The microstructure uniformity and stability of the foams made from ARB precursors depend on the surface concentration and morphology of the foaming agent as well as on the foaming temperature.

#### *Acknowledgement*

This work was supported by funding from the Public Agency for Research and Development of the Republic of Slovenia, as well as the Impol Aluminium Company and Bistral d.o.o., from Slovenska Bistrica under contract No. 2410-0206-09.

#### **References**

- [1] N. Tsuji, Y. Saito, S. H. Lee, Y. Minamino, *Adv. Eng. Mater.*, 5 (2003) 5, 338
- [2] Y. Saito, H. Utsumonia, N. Tsuji, T. Sakai, *Acta Mater.*, 47 (1999), 579
- [3] K. Kitazono, E. Sato, K. Kuribayashi, *Scripta Mater.*, 50 (2004), 495
- [4] K. Kitazono, E. Sato, *Materials Science Forum* 475-479 (2005), 433
- [5] L. E. G. Cambonero, J. M. R. Roman, F. A. Corpas, J. M. R. Prieto, *Journal of Materials Processing Technology*, 209 (2009), 1803
- [6] D. P. Papadopoulos, H. Omar, F. Stergioudi, S. A. Tsipas, N. Michailidis, *Colloidal and Surfaces A: Physiochem. Eng. Aspects* 382 (2011), 118
- [7] V. Gergely, D. C. Curran, T. W. Clyne, *Composites Science and Technology*, 63 (2003), 2301
- [8] V. Kevorkijan, S. D. Škapin, I. Paulin, B. Šuštaršič, M. Jenko, *Materials and technology* 44(2010) 6, 363
- [9] US Pat. No. 7.452.402 issued on November 18, 2008